Mapping mean annual river discharges: geostatistical developments for incorporating river network dependencies

Eric Sauquet

Author-produced version of the article published in Journal of Hydrology
2006, 331(1-2),300-314.
The original publication is available at http://www.sciencedirect.com/
doi : 10.1016/j.jhydrol.2006.05.018

SAUQUET E., 2006. Mapping mean annual river discharges: geostatistical developments for incorporating river network dependencies. Journal of Hydrology, 331, 300– 314

Mapping mean annual river discharges: geostatistical developments for incorporating river network dependencies

ERIC SAUQUET

Cemagref, Hydrology - Hydraulics Research Unit, 3 bis quai Chauveau CP220, 69336 Lyon cedex 09, France

e-mail: sauquet@lyon.cemagref.fr

Abstract Estimations of hydrological descriptors are required for studying links between river flow and ecological processes at different scales, from local scale at which biological and/or water quality data are usually available, to larger scale for sustainable development purposes. The study of regional hydrology has seen significant advances in recent years due to new developments in statistics, environmental database access, and calculating capabilities. Nevertheless, theoretical difficulties for mapping and for estimating river regime characteristics at ungauged locations remain because of the nature of the variable under study: river flows are related to a specific area, i.e. the drainage basin, and are hierarchically organized in space through the river network with upstream-downstream dependencies. This presentation aims at describing a method for producing choropleth maps of average runoff and computing mean discharge along the main river network. The approach applied to mean annual runoff is based on geostatistical interpolation procedures coupled with empirical relationships and is illustrated by an application to assess water resource in France. The performance of the developed approach is tested against two other geostatistical methods (ordinary kriging and residual kriging). This study concludes that the classical approaches for interpolation can be improved by explicitly introducing hydrological properties of the mapped variable.

Keywords: kriging, interpolation, runoff, discharge, river network

1. Introduction

Various methods have been developed for mapping runoff features ranging from manual contouring to automated procedures. Maps produced manually (Gannett, 1912) were published first since calculating capacities were limited at the time they were created but they are still in use in the 90's (Krug *et al.*, 1990). The manual procedures, time consuming and by definition subjective (no confidence level can be computed), have been progressively abandoned as new technologies, e.g. geographical information systems, emerged. Empirical relationships between streamflow and land use, geomorphology and climate have received wide attention for several decades (Solomon *et al.*, 1968; Liebscher, 1972; Dingman, 1981; Hawley and Mc Cuen, 1982; Gustard *et al.*, 1989; Herschy and Fairbridge, 1998; Vogel *et al.*, 1999). Such formulas have been usually established by multivariate regional regression. Drainage area and precipitation are by far the most significant explanatory variables and consequently are found in numerous published works. Other basin characteristics (annual maximum temperature, basin perimeter, slope and length of the main channel, mean basin elevation, gauging station co-ordinates, area controlled by lakes, etc.) may be incorporated but their relevance in relationships is usually not warranted when a new region is examined. The empirical formulas are only valid within the region where fitting was achieved.

Besides, rather than estimating one single characteristic, hydrologists may simulate the whole hydrological behaviour over the domain applying lumped rainfall-runoff models (Jutman, 1995) or more physically based models (Bishop *et al.*, 1998). Several difficulties may restrict the application of this approach:

- a large set of basins is required to calibrate the models against records;
- the spatial coverage of rainfall conditions the inputs of the models and their efficiency in simulating discharge time series;
- the model parameters vary spatially but are not suited to regionalisation since their link to the physical parameters of the basin is not well known.

The question of selecting an efficient interpolation method is then assigned to other variables: the climatic inputs and the internal parameters of the hydrological models.

An alternative is given by objective methods (Gandin, 1960, Matheron, 1965) that aim at rebuilding stochastic fields using a sparse observation network. These methods differ by the hypothesis on the interpolated variable to be satisfied (homogeneity, isotropy) and the function used to express spatial dependencies. Estimation at an ungauged location is achieved by weighting data observed at neighbouring locations. These approaches have been previously and successfully applied to map point processes in hydrology. The literature is less extensive and more recent about discharge characteristics (Villeneuve *et al.*, 1979; Gottschalk, 1993; Huang and Yang, 1998; Gottschalk and Krasovskaïa, 1998; Merz and Blöschl, 2005). Two key-points make the application of geostatistics to runoff characteristics delicate: the definition of a relevant distance between basins and the underlying assumptions of the variables to be regionalised. Thus, Gottschalk (1993) suggested replacing distance and covariance for points by specific distance and covariance for drainage basins. The fact that runoff is to be integrated to streamflow is explicitly included in the interpolation scheme. These concepts were later extended for estimating mean annual water depths on elements of a partition of a large basin (Sauquet *et al.*, 2000a). The procedure involves spatial redistribution of the annual volume

produced at the outlet of the large basin. This configuration is restrictive, as all the mouths to the sea are not gauged. Moreover, spatial homogeneity in runoff features is required to apply this approach.

The main objective here is to extend and generalize the geostatistical procedure suggested by Sauquet *et al.* (2000a) to account both for spatial heterogeneity and river network dependencies. This work is motivated by an application on a national scale to answer some basic questions related to the European Water Framework directive. This paper is divided into four sections. Section 2 focuses on methodological aspects. First, the basic equations of kriging are presented. The developed approach, called "hydro-stochastic" is then introduced to account for the fact that gauging-station data represent flows contributed by drainage areas with varying sizes and characteristics rather than point values. The section focuses on data and distance to be considered. Section 3 illustrates the application to a vast dataset in France, including more than 950 gauging stations. Runoff estimates were computed for more than 6000 elements of different size that partition France. We quantify the performance of the proposed framework in Section 4. Several efficiency coefficients are calculated. This uncertainty analysis compares the reliability of the results to the ones obtained applying two other geostatistical but less sophisticated methods. Last, conclusions are given in Section 5.

2. The interpolation system: an hydro-stochastic approach

2.1 The kriging equations

Kriging is a procedure used in geostatistics to predict unknown values from data observed at known locations. With kriging, the estimated value $z(\mathbf{u})$ at location $\mathbf{u}$ is a linear combination of observed values $z(\mathbf{u}_i)$, $i = 1,\ldots,N$ located in the neighbourhood of $\mathbf{u}$:

$$z(\mathbf{u}) = \sum_{i=1}^{N} \lambda_i(\mathbf{u}) z(\mathbf{u}_i) \quad (1)$$

where the weights $\lambda_i(\mathbf{u}), i = 1, \ldots, N$ ensure the unbiasedness of the estimator and are computed by minimising the estimation variance. Under the assumption that the process is homogeneous in space, this leads to the resolution of the following linear system known as "ordinary kriging system" (Matheron, 1965):

$$\begin{cases} \sum_{j=1}^{N} \lambda_j(\mathbf{u}) \gamma\left(\left|\mathbf{u}_i - \mathbf{u}_j\right|\right) - \mu(\mathbf{u}) = \gamma\left(\left|\mathbf{u}_i - \mathbf{u}\right|\right), i = 1, ..., N \\ \sum_{j=1}^{N} \lambda_j(\mathbf{u}) = 1 \end{cases} \quad (2)$$

where $\left|\mathbf{u}_i - \mathbf{u}_j\right|$ denotes the Euclidian distance between $\mathbf{u}_i$ and $\mathbf{u}_j$, $\mu(\mathbf{u})$ is the Lagrangian multiplier accounting for the constraint of unbiasedness and γ is the theoretical model fitted to the experimental semi-variogram defined by:

$$\hat{\gamma}(h) = \frac{1}{2N(h)} \sum_{i,j}^{N(h)} \left(z(\mathbf{u}_i) - z(\mathbf{u}_j)\right)^2 \quad (3)$$

where $N(h)$ is the number of couples of observations separated by a distance h. Permissible models of semi-variogram are tested and compared graphically to the empirical semi-variogram. The selected function for γ is the one giving graphically the best fit.

2.2 A relevant distance to measure proximity between geographical sectors

This approach is of wide use for interpolation of meteorological fields (Creutin and Obled, 1982; Dingman *et al.*, 1988; Goovaerts, 2000) but needs to be modified for runoff features since the runoff observations are related to specific areas rather than to points. In particular, a relevant distance between pairs of basins has to be defined. Huang and Yang

(1998) and Merz and Blöschl (2005) allocate the representative value of the runoff depth to the centre of gravity of the basin and thus chose the distance between centres of gravity. Unfortunately this distance may bring together basins with significantly different river flow regime, particularly when basins are nested. We can demonstrate that this kind of configuration is not so uncommon in the data set (Fig. 1): let us consider two French basins - the Garonne River at LAMAGISTERE (32 350 km²) and one of its tributaries, the Girou River at CEPET (522 km²). The centres of gravity of the two catchments are 3.6 km apart, but river flow regime is distinct. The Garonne River with a fraction of water originating from the Pyreneans Mountains shows a transitional flow regime between nival and pluvial patterns, while the Girou River has a typical rainfall fed flow regime. If no hydrological information is available along the Garonne River nearby LAMAGISTERE, the kriging technique using distance between centres of gravity - erroneously - assigns a disproportionate weight to the Girou River in the runoff prediction at LAMAGISTERE. Hence there is a risk of including two nested basins with a distance between their centres of gravity equal to zero in the linear system and in this case, kriging system has no solution. Solutions do exist when dataset includes observations collected multiple times at the same location (Goovaerts *et al*., 2005). The kriging matrix they proposed is not directly appropriate in our context, as two or more streamflow records are related to two or more distinct supports that, by chance, have the same centre of gravity. The effects of the support on variance and semi-variogram have been extensively examined (e.g. Wackernagel, 1995; Bras and Rodriguez-Iturbe, 1993). On the other hand, the question concerning the appropriate choice of a distance measure between supports with different sizes is still open and the drawbacks of using distance between centres of

gravity have been rarely pointed out. Gottschalk (1993a) suggested a measure of distance, named Ghosh distance (Ghosh, 1951; Matérn, 1960), taking into account both the river network and the drainage basins. This distance h between two geographical sectors S_1 and S_2, of areas respectively equal to A_1 and A_2, is defined by the average distance between all the couples of points within the two sectors:

$$h(S_1, S_2) = \frac{1}{A_1 A_2} \int_{\mathbf{u}_1 \in S_1} \int_{\mathbf{u}_2 \in S_2} |\mathbf{u}_1 - \mathbf{u}_2| \mathbf{du}_1 \mathbf{du}_2 \quad (4)$$

These sectors A_1 and A_2 could be basins or sub-basins to accomplish the spatial analysis of runoff data. This distance allows better identification of the spatial structure of runoff (Gottschalk, 1993a). Adopting an assumption of local second-order stationarity of the runoff process, a kriging system may be established and resolved (Gottschalk, 1993b).

The Ghosh distance (equation 4) is used in all steps of the interpolation framework in the hydro-stochastic approach, that means this distance replaces the classical Euclidian distance. Some links exist between these two distance measures. The following inequality between these two distance measures is verified:

$$h(S_1, S_2) \geq |\mathbf{u}_{G1} - \mathbf{u}_{G2}| \quad (5)$$

where $\mathbf{u}_{g_i}$ denotes the coordinates of the centre of gravity of basin S_i. $|\mathbf{u}_{G1} - \mathbf{u}_{G2}|$ converges towards $h(S_1, S_2)$ when S_1 and S_2 are not over-lapping and have small size or when S_1 and S_2 are distant, i.e. for large values of $|\mathbf{u}_{G1} - \mathbf{u}_{G2}|$.

2.3 Accounting for spatial heterogeneity

The runoff characteristic $z_q(A)$ related to the element A is calculated using the weighted linear combination of N observed values $z_q(A_i)$, $i = 1,\ldots,N$:

$$z_q(A) = \sum_{i=1}^{N} \lambda_i(A) z_q(A_i) \quad (6)$$

If spatial homogeneity is valid, ordinary kriging can be applied and z_q are directly estimated by resolving the linear kriging system (equation 2). When spatial homogeneity is rejected, an empirical formula linking the spatial features z_q to K basin characteristics is fitted:

$$z_q{}^*(A) = g(X_1(A), X_2(A), ..., X_K(A)) \quad (7)$$

where X_i, i= 1,…,K are mapped basin characteristics and the deviation ε_q is calculated at each gauging station:

$$\varepsilon_q(A) = z_q{}^*(A) - z_q(A) \quad (8)$$

ε_q is supposed to satisfy the intrinsic hypothesis, the related empirical and theoretical semi-variograms are estimated. Errors ε_q are interpolated using (equation 2) and z_q* deduced from the maps of X_i, i= 1,…,K. The combination of the map of ε_q and the map of z_q* gives finally an estimate of z_q for each target area.

This approach is known as “residual kriging” in the geostatistical literature and referenced as “georegression” in some applications in hydrology (Faulkner and Prudhomme, 1998; Merz and Blöschl, 2005) when g is a first order polynomial. Including basin descriptors in the empirical formulas is a way to account for the fact that streamflow data result from processes operating over the whole basin.

2.4 Variables under study

Traditionally when mapping river discharge, the variable under study introduced in the interpolation procedure is runoff observed at the outlet of gauged basins. Handling this variable has one major drawback. When runoff from nested gauged basins is directly

used in the interpolation scheme, information on the headwaters is introduced several times in the data set due to the over-lapping drainage area. This redundancy may bias the spatial analysis.

To remedy such a problem, we suggest to cope with values calculated by subtracting the discharge(s) measured upstream from the value observed downstream. This data processing is the first step of the area weighted average gridded mapping method (Arnell, 1995). The proposed interpolation framework deals with runoff $q\tilde{a}$ generated by each portion of basin between two or more gauging stations or uppermost headwaters of basins where no records are available upstream. The supports in equation 4 are thus basins or sub-basins. Thus, we assess intermediate lateral river inflow and expect to distinguish more accurately areas with high runoff and areas with low runoff. Lastly, to eliminate scale effect within the data set due to the size of the basin, runoff $q\tilde{a}$ generated by sub-basin is expressed in mm/yr.

2.5. Estimating discharge along the river network

The kriging procedure suited to runoff characteristics enables one to estimate runoff for any delineated element. A special case is when runoff is estimated on elements of a partition of the study area ΔA_i, $i = 1,\ldots,M$, considered as fundamental units (i.e. M non-overlapping target elements with small size that form the whole domain). Estimations are provided by aggregation along the river network (Estrela *et al.*, 1997). The annual discharges qa generated by the area upstream to the location **u** are the sums of the runoffs $q\tilde{a}$ generated in all fundamental units ΔA_i flowing into that location **u**:

$$qa(\mathbf{u}) = \frac{1}{A} \sum_{\Delta A_i \subset A} q\tilde{a}(\Delta A_i)\Delta A_i \qquad (9)$$

where A is the drainage area at location **u** and discharge are expressed in mm/yr.

Lastly corrections with respect to karstic influences are proposed on discharge estimates when flows are recorded at the resurgence affecting downstream discharge or when the location of sink holes is known. In the first case, the measured value is introduced as local inflow in the map of $q\tilde{a}$. In the second case, the outflow is estimated by the difference between observed value and theoretical value deduced from the map by integration (equation 9) and thereafter introduced in the map of $q\tilde{a}$. When no precise information is available, the outflow or inflow may be evenly distributed along the river between two gauging stations delineating the area of possible sinks holes or resurgence.

The fundamental units of the partition define the finest level of detail that can be achieved for describing runoff variability. To limit inconsistency, discharge cannot be computed accurately along all the river network. Two cases are considered:

- when rivers have their source in a fundamental unit ΔA, discharge estimates are only given for basins larger than ΔA;
- when rivers run cross a fundamental unit ΔA, discharge estimates are given along the portion of the river network located inside ΔA.

3. Application

A case study is proposed in connection with the European Water Framework directive that aims at improving ecological quality of surface waters. To achieve this main objective in France, there is first a need to evaluate hydrological characteristics along the river network. Indeed runoff pattern may explain and influence the structure and functioning of aquatic ecosystems. Results are detailed for a part of France – the Meuse River basin - to exemplify the procedure when dealing with monitored karstic areas.

3.1. The study area

Climate in France is quite diverse with mean annual precipitation ranging from 300 mm/yr in the French lowlands of the Rhine River to more than 2500 mm/yr in the mountainous regions (Alps). Precipitation, air temperature and elevation variability governs mainly the spatial diversity of river flow regimes (Fig. 2): the glacier/snowmelt-fed regimes are found in the mountainous part of France (high altitude rivers in the French Alps and French Pyreneans) (1-2 in Fig. 2) in contrast to the northern and western part of France under maritime temperate climate influences, where pluvial regime governed by rainfall and evaporation is dominant (alluvial plains of the Seine basin and rivers from Brittany) (3 in Fig. 2). In the South of France, Mediterranean climate with hot and dry summer prevails and small rivers experience severe low flows in August and intense rainy events in autumn generating "flash floods" (4 in Fig. 2). Lastly reservoir storage, interbasin water diversion or other forms of regulation may alter significantly natural flow regime with a reduction of both annual water availability and variability from month-to-month (5 in Fig. 2).

3.2. Drainage basin delineation

An exhaustive description of the river network is required to compute runoff and physiographic parameters for each gauged (sub-)basin and to derive characteristics of the topological river patterns including the downstream-upstream dependencies and the distance between couples of gauged (sub-)basins. The linkage between all these (sub-)basins is examined in the spatial analysis and the emerged properties are thereafter introduced in the interpolation procedure. As no digitised drainage basin areas were available, the river network has been extracted from a raster digital elevation model (DEM) with 1×1 km cells using the software HydroDEM (Leblois and Sauquet, 2002).

The DEM is a re-sampling of the Global 30 Arc Second Elevation Data Set of the U.S. Geological Survey, freely available on the Internet. Combining the elevations from the DEM and a land cover database with the derived drainage pattern enable to calculate some basin attributes of interest (drainage area boundary, hypsometric curve, location of the centre of gravity, proportion of basin area as forest, etc.). To test the accuracy of the derived river network, a geometrical tolerance criterion based on the difference between actual and estimated basin areas (Sauquet *et al.*, 2000b) was calculated for 2517 French gauging locations of more than 40 km² where drainage area is known. We consider that the basin boundaries are correctly reproduced if:

$$|A^* - A| \leq \chi \cdot d_0 \qquad (10)$$

where A denotes the actual area, A^* the area derived from the DEM analysis, χ the perimeter of the basin and d_0 the resolution of the DEM. Thus, we tolerate a maximal error of one grid cell along the boundary of the drainage basin. Here the actual shape of each basin is unknown. We considered the most critical situation: disk is the geometric shape with the smallest ratio χ/A. Thus we fixed χ on the perimeter of an equivalent round basin with area A:

$$|A^* - A| \leq 2\sqrt{A\pi} \cdot d_0 \qquad (11)$$

This criterion is more relevant than a subjective tolerance threshold - expressed as a percent of the actual area - since it accounts for both the size of the basins to be delineated and the spatial resolution of the DEM. The constraint imposed by the criterion stated on (equation 11) is rejected for only 55 of the 2517 gauged basins (Fig. 3). The most significant deviations are found in chalky sectors or rivers with large diversion. The quality of the river network derived from the DEM delineates drainage basins accurately

and average distances between sub-basins and mean basin elevation may be computed with a high level of confidence.

3.3. Streamflow database

The French hydrological database HYDRO offers time series of observed and reconstructed natural monthly discharges. To ensure temporal consistency and to provide reliable runoff estimates, a common observation period of continuous records (1981 to 2000) was used. In France, water year starts the 01-September and ends the 31-August of the following year. The total data set consists of 965 gauged basins with minor human impact, with minimal gaps in the data record (at least 17 years of records within the time period 1981-2000) and with high quality data (Fig. 4). Incomplete time series were filled by linear correlation between monthly discharges at nearby stations established on the common period of records.

The drainage areas vary in size from 11.5 to 111 570 km². Within these 965 stations, a group of 67 basins with strong control by karst aquifers was constituted (karstic data set). The stations of the karstic data set were first withdrawn because of the uncertainties on their drainage areas. Incorporating water depths of these basins may bias the derivation of the model g (equation (7)). Drainage areas downstream to these karstic sectors and their runoff estimation have been introduced in the data set.

Long-term averages $q\tilde{a}(A_i)$ generated by each sub-basins area A_i, i=1,…, N are computed from monthly data. Mean annual runoff for the 898 sub-basins ranges from 70 mm to more than 1860 mm with an average of 460 mm per year (Fig. 5). The lowest values are found in the southern part of the Rhone Valley whereas the highest ones are located in the Alps.

3.4. Results

In this application, commonly used characteristic or classification system derived from physical properties including soil type, hydrogeology, … and climate characteristics were not available. The only information we used is given by the streamflows observed at gauging stations, topography depicted by the DEM and derived drainage network. Thus, the list of basins characteristics is reduced to one descriptor: the mean basin elevation. Indeed, at a large scale, altitude is the factor with the greatest influence, above geology and land-use, as it contains information on climate and explains most of the spatial heterogeneity in rainfall fields. Moreover we suppose that spatial heterogeneity was mainly due to altitude and that deviations from the empirical formulas g fitted to observations reveal specific geological conditions, micro-climate, effect of terrain barriers on precipitation…

Our application considers a wide geographical domain (552 000 km²). France is divided into ten major geographic areas that are hydrologic divisions based on topography. Runoff was estimated using a partition of the study area into 6189 elements $\Delta A_i, i = 1,...,M$ with M= 6189. This target partition is one of the layers of the French database CARTHAGE (CARtographie THématique des AGences de l'eau et du ministère de l'Environnement; thematic cartography of the Water Agencies and the Ministry of the Environment). These 6189 elements have different sizes from 0.01 km² to 3753 km². The median size is equal to 67 km². Some rivers have their spring outside France (e.g. Rhone) or flow cross other countries. Runoff estimates were provided on headwater and sub-basins outside the boundaries, but were intentionally omitted in the maps that focus on France. All of these areas are fundamental units and enable us estimating runoff along the

river network by re-aggregation. For each of these elements, mean elevation was calculated. Calculations were carried out for the whole of France but we show hereafter the results for four specific regions (1, 4, 6, 10) that are subject to distinct climatic and geologic influences (e.g. Region 4: granite and temperate climate for Brittany, Region 10: chalk and Mediterranean climate for the South of the Rhone Valley, Region 1: heterogeneity in geology and topography (chalk in the lowlands of the alluvial Rhine floodplain and granite in the Vosges Mountains).

For each major sector, nearby outside stations were added to the subset of stations located within the region in order to guarantee continuity on both sides of the boundaries (Table 1). This number of additional stations depends on the location of the region (it can be for instance region partially surrounded or not by ocean, by another country with no neighbouring station available) and on the large extent of areas underlain by chalk. For Region 8, we can notice a high quantity of additional stations compared to the total number of stations included in the interpolation scheme (Table 1). This disproportion is not due to a relative poor density of the monitoring network but rather due to the predominance of karst terrain along the river network that reduces the number of usable stations (Fig. 5).

Regression analysis was performed over each region. Mean elevation over gauged sub-basins was taken as the explanatory variable to estimate the related mean annual runoff $q\tilde{a}$. Fig. 6 shows the goodness of fit of the equations for the Regions 1, 4, 6 and 10. Hypsometric curves were derived for each region (Fig. 7). Table 1 summarizes the regression models for the ten regions in France. The slope and the intercept differ from one region to another. The determination coefficients for the ten equations range from 5%

to 63%, indicating a weak to moderate correlation between runoff and elevation. According to Fisher test, the determination coefficients differ significantly from zero at 1% risk level for all regions, but Region 2 and Region 4. When region topography is contrasted (Fig. 7), the link between orography and runoff characterised by the determination coefficient is pronounced. Elevation was considered as a major factor influencing runoff for eight of the ten regions ($R^2 > 0.20$). These eight regions for which regression coefficient is significantly different from zero are partially covered by mountainous areas and runoff tends to rise with increasing elevation. This is a natural phenomenon due to orographic effect that induces the enhancement of precipitation by the presence of mountains. Spatial homogeneity was rejected for these regions. The elevation effect is well pronounced in these eight sectors and, consequently, even a locally stationary regionalisation model is judged inadequate. The deterministic component is subtracted from observed runoff values to obtain residuals, variables to be interpolated. Lastly the hydro-stochastic approach was applied to the variable $q\tilde{a}$ for Region 2 and Region 4 and to residuals for the other regions.

Spatial analysis was achieved for each region using equation 4 for distance computation. The exponential model gives an acceptable fit to the experimental semi-variograms (Fig. 8):

$$\gamma(h) = C_0\left[1 - \exp(-h/a)\right] \quad (12)$$

The fitted parameters are given in Table 2. a is the spatial scale coefficient. A high value of a is an evidence for a strong spatial correlation between distant observations. The estimated value a varies according to the region from 20 km to 70 km. In the data set, there is no obvious link between a and the topography. C_0 is the sill of the semi-

variogram and has to be compared to the variance of the random function. The semi-variogram for Region 10 displays a hole effect typical of periodic phenomena (Journel and Huijbregts, 1978). The sill is reached at 220 km and then the semi-variograms dips to a local minimum at around 320 km. The well-pronounced hole effect is connected to the presence of two mountain chains (Cévennes, Alps) roughly distant from 200 km on both sides of the Rhone Valley. In these two sectors, the regression formula systematically underestimates mean annual runoff and creates areas of high positive residual surrounded by areas exhibiting lower residuals.

The map of mean annual runoff is consistent with its expected spatial pattern (Fig. 9). The largest runoff values (more than 2000 mm/yr) are found in the uppermost part of the mountainous sectors (Vosges, Alps, Jura, Pyreneans), whereas the lowest ones (less than 50 mm/yr) are located in the east part of France (alluvial plain of the Rhine River) and in the Southern lowlands. The higher quantities of runoff are provided by the Alps, which is considered as the "water tower of France".

The areal average runoff over France is computed and equal to 370 mm/yr. The related proportion of river runoff to precipitation in France is close to 40%, which is a commonly adopted value under temperate climate (Herschy and Fairbridge, 1998).

3.5. A more detailed application to the Meuse River basin

The algorithm for deriving discharge along the river network accounting for subterranean diversion is exemplified on the French part of the Meuse River basin (7 800 km²) (Fig. 10, Fig. 11). The Meuse River rises in the Plateau de Langres, at 384 m above the sea level, runs successively across Belgium and the Netherlands before flowing into the North Sea near Rotterdam. The total length of the river network is 950 km and the

geology is mainly marl (chalk and clay). The flow regime assigned to the Meuse River and its tributaries is predominantly pluvial according to Pardé's classification (Pardé, 1955). The Aroffe River disappears by Gémonville (45 km²), flows through subterranean faults and reappears close to Barisey (180 km²) and finally joins the Meuse River at Rigny St Martin (265 km²). A proportion of water is diverted toward the Moselle River but the location of the water reappearances is not well known.

First, discharges along the Aroffe River were calculated using equation (9) without considering karst. Runoff was evaluated to 348 mm/yr (2.18 m^3/s) at the gauging station VANNES-LE-CHATEL (198 km²) (Fig 10, Fig. 11.a). This value is compared to the observed one 127 mm/yr (0.80 m^3/s). The total runoff volume diverted toward the neighbouring Moselle basin was calculated by difference: 43.8 hm^3 per year, and on average, 1.38 m^3/s from the Aroffe River flows into the Moselle basin. This value is subtracted to the discharge estimated downstream to Gémonville, a location along the Aroffe River now considered as the sinkhole (Fig. 11.b). Then the final map of mean annual discharge is derived from the DEM and the map of annual runoff modified by subterranean influences. Results are shown along the river network constraint by the resolution of the partition (Fig. 11.c, Fig 11.d, Fig. 12). Subsurface runoff has now disappeared between Vannes-le-Chatel and Barisey. Without any information about the location of the resurgences of the upstream part of the Aroffe River, it was not possible to modify objectively runoff estimations for the Moselle River.

4. Analysis of predictive performance

In this paragraph, a jack knife procedure is applied for comparing the accuracy of three interpolation techniques including the hydro-stochastic approach and two other

geostatistical methods. Stress is put on the specific procedure for the hydro-stochastic method, which requires two steps before assessing efficiency: firstly runoff estimation by interpolation procedure and secondly aggregation along the river network to derive mean annual flow.

4.1 Method

The interpolation procedure is assessed by jack-knife. Computed indices of reliability are compared to those obtained for two geostatistical interpolators: ordinary kriging and residual kriging, both methods using distance between centres of gravity and mean annual runoff *qa* observed at each gauging station without the pre-processing suggested by Arnell (1995). The stationarity property does not hold for all of the regions but only for two of them for which ordinary kriging is appropriate (Region 2 and Region 4). Nevertheless, ordinary kriging was applied to measure the benefit of incorporating external information in the algorithm.

The predictive performances was conducted for each region. . The procedure consists in withdrawing in turn 10% of the gauging stations selected randomly from the original dataset. The additional stations from nearby regions were not involved in this removal procedure. Runoff was estimated at the withheld stations using the three methods and the remaining stations. These steps are repeated ten times for each region, to exclude each station exactly one time. In the hydro-stochastic method, the slope and the intercept of the regression $q\tilde{a}$ versus mean elevation and the exponential model for the semi-variogram has to be adjusted to the remaining stations. First runoff generated by the elements of the partition is calculated by interpolation, then the mean annual flow at each gauging station is obtained by aggregation along the river network.

The performance of each method is examined using the following criteria: the slope, the intercept and the determination coefficient of the regression between estimates and observations, the root mean square error (*RMSE*) which measures the average difference between observation and estimation:

$$RMSE = \sqrt{\frac{1}{n}\sum_{i=1}^{n}\left(qa(i) - qa_{est}(i)\right)^2} \quad (13)$$

and the mean of the absolute relative error (%):

$$MARE = \frac{100}{n}\sum_{i=1}^{n}\left|\frac{qa(i) - qa_{est}(i)}{qa(i)}\right| \quad (14)$$

where n is the number of basins considered for the uncertainty analysis, qa and qa_{est} are respectively the observed data and the predicted value for site i (in mm/yr). The dimensionless index *MARE* was chosen to remove the impact of the differences in the runoff magnitude in the performance evaluation diagnosis. These indices investigate several aspect of model performance and the most effective method will be assessed according to their values.

Since the estimation by aggregation is scale-dependent with the resolution of the partition, we concentrated on a subset of basins among the withheld gauging stations for evaluation purposes. Only estimations for withdrawn basins, which overlap at least one element of the partition, should be compared to observations. Stations from the karstic data set are not involved in the uncertainty analysis. 668 from the 898 gauging stations were considered.

4.2. Results

Fig. 13 illustrates the performance of the three methods for four regions (1, 4, 6 and 10) and suggests that the approaches are efficient and comparable in their predictive ability.

The deviation to the one-to-one line is slightly noticeable when all the stations are considered (Fig. 14.a). Points are evenly scattered around the one-to-one line. Hence no under or over-estimating tendency within the tested approaches is obviously detected.

The cumulative distribution functions of the differences in runoff suggest that the worst method was ordinary kriging (Fig. 14.b). This is supported by the computed indices of Table 3 that gives the results of the jack-knifing approach for each region. The last line of Table 3 reports the performance indices combining all the stations of the ten regions. The regression lines deviate slightly from the one to one line: slope is ranging from 0.64 (Region 9 using ordinary kriging) to 1.02 (Region 2 using ordinary kriging). The determination coefficients vary between 0.72 and 0.97 except for the hydro-stochastic approach applied to Region 2 (R^2= 0.60). Scores are poor for Region 2, whatever the regionalisation technique. This is likely due to the small number of stations (14) and the effects of urban and industrial development, which are much greater in that region than in any other.

We can notice that there is no need to compute an overall rank score as the one defined by Shu and Burn (2004). If one method is assumed the best according to one index, this method is quite systematically the best according to the others indices. The hydro-stochastic approach was superior according to all measures of efficiency for 7 of the 10 regions. In the three regions (2, 4, 8) where the hydro-stochastic approach was not clearly superior, its performance did not differ greatly from the other methods. When all 668 stations are considered, the hydro-stochastic approach is superior according to all efficiency indices. Furthermore, the MARE for the hydro-stochastic approach varies only

slightly around 12% (between 8% and 17%), whereas the spread of that index for the other methods is considerably larger.

Ordinary kriging performs relatively well even if the stationarity property is rejected (Region 1). The geographical proximity of centre of gravity can be used to assess runoff with an acceptable level of confidence. These results strengthen conclusions of other works on flood characteristics by (Merz and Blöschl, 2005) and on mean annual runoff (Sauquet *et al*., 2000a). The gain obtained by including the elevation is observed in most cases (for eight of the ten regions). Residual kriging using distance between centres of gravity is finally ranked 2nd.

For further investigation we decided to analyse results from the performance comparison on different classes of basins. We divided the data set of 668 gauging stations into six subsets according to their size:

- Class 1: basins with drainage area between 50 and 500 km²;
- Class 2: basins with drainage area of more than 50 km²;
- Class 3: basins with drainage area of more than 100 km²;
- Class 4: basins with drainage area of more than 500 km²;
- Class 5: basins with drainage area of more than 1000 km²;
- Class 6: basins with drainage area of more than 5000 km².

Absolute errors were computed and results were summarised by box plots (Fig. 15). Using classes of basin areas reveals that estimates from the three approaches did not differ substantially for the 402 small basins of Class 1. The marked differences concern Class 5 and Class 6, including respectively 152 basins and 42 basins. Fig. 15.a shows that the performance ability of the hydro-stochastic approach is scale dependent: the larger the

basin, the lower the prediction error considering all the statistics from the 25% percentile to the maximum absolute deviation. The median absolute error is 43 mm/yr for Class 1 and 8 mm/yr for Class 6. Errors have wider spread when ordinary kriging is applied and the range of error remains constant with the size of the basin (Fig. 15.c). Maximum error of residual kriging using distance between centres of gravity diminishes with the area but not the median (Fig. 15.b). The well-pronounced decrease of the error with the drainage area explains in part the better performance of the hydro-stochastic approach. Aggregation along the river network is a way to account for the anisotropy in discharge characteristics induced by the over-lapping areas. In that way, calculating discharge using continuity equation (i.e. the river network dependencies) ensures better estimations for large basins than algorithms based only on proximity between stations.

5. Conclusions

One technique for mapping long term mean runoff describing water resource at basin scale is presented. It is based on objective methods specially developed to account for the related drainage basin supporting areas and the hierarchy in the discharge data imposed by the structure of the river network. The proposed procedure ensures consistency in space: the continuity equation is fulfilled by aggregation along the water path to derive discharge. Thus, inconsistencies are avoided when two main rivers flow together. The uncertainty analysis demonstrate that classical approaches for interpolation give acceptable results but can be slightly improved by introducing hydrological properties of the variable under study in the mapping procedure. The mean absolute error on discharge is equal to 12%, and this value for a quite heterogeneous area indicates that the algorithm gives useful estimates..

This framework can be applied to other runoff characteristics but these variables should be average runoff over time. The disaggregation approach is not suited to T-year return period flood quantiles that have not the properties to add themselves downstream to a confluence. This property may be accepted as a rough hypothesis for mapping low flow characteristics due to the large geographical extent of drought events but need to be confirmed by observations.

Other basin characteristics can be introduced in the empirical relationships to compute thereafter residuals with respect to the spatial heterogeneity. Here, we have followed the Laplace principle of "insufficient reason" (i.e. “if you have no justified reason, make it simple”) and only one explanatory variable was considered in the empirical formula: the mean elevation. No meteorological data were involved in the estimation procedure. Thus, the map of runoff we derived might be compared objectively to the maps of rainfall and evapotranspiration for the same period to detect and correct easily spatial inconsistencies by combining the unrelated maps and to grasp the full view of the water budget on a national scale.

Acknowledgements

The authors gratefully acknowledge support, either as fund or data, by the French Ministry of Ecology and Sustainable Development. The paper has been improved by helpful comments from Pr. Lars Gottschalk, Dr. I. Krasovskaia, Dr. M.H Ramos and the two reviewers.

References

Arnell, N.W., 1995. Grid mapping of river discharge. Journal of Hydrology 169, 39 - 56.

Bishop, G.D., Church, M.R., Aber, J.D., Neilson, R.P., Ollinger, S.V., Daly, C., 1998. A comparison of mapped estimates of long-term runoff in the northeast United States. Journal of Hydrology 206, 176-190.

Bras, R. L., Rodriguez-Iturbe, I., 1994. Random Functions and Hydrology, Addison Wesley, 1985; new printing, Dover Publications, New York.

Creutin, J.D., Obled, C., 1982. Objective analysis and mapping techniques for rainfall fields an objective comparison. Water Resources Research 18, 413-431.

Dingman, S.L., 1981. Elevation: a major influence on the hydrology of New Hampshire and Vermont, USA. Hydrological Sciences Bulletin 26(4): 399-413.

Dingman, S.L., Seely-Reynolds, D.M., Reynolds, R.C., 1988. Application of kriging to estimating mean annual precipitation in a region of orographic influence. Water Resources Bulletin 24, 329-339.

Estrela, T., Quintas, L., Alvarez, J., 1997. Derivation of flow discharges from runoff maps and digital terrain models in Spain, FRIEND'97 - Regional Hydrology : Concepts and Models for Sustainable Water Resource Management. AISH Publication n°246, Postojna (Slovenia), 39-48.

Faulkner, D.S., Prudhomme, C., 1998. Mapping an index of extreme rainfall across the UK. Hydrology and Earth System Sciences 2, 183-194.

Gandin, L.S., 1960. On optimal interpolation and extrapolation of meteorological fields (in Russian). Trudy GGO vyp.287: 35-41.

Gannett, H., 1912. Map of the United States Showing Mean Annual Runoff. In: Surface Water Supply of the United States, 1911, U.S. Geological Survey, Water Supply Papers, n° 301-312, Government Printing Office, Washington, DC, pt. II.

Ghosh, B., 1951. Random distances within a rectangle and between two rectangles. Bull. Calcutta Math. Soc. 43.

Goovaerts, P., 2000. Geostatistical approaches for incorporating elevation into the spatial interpolation of rainfall. Journal of Hydrology 228(1-2), 113-129.

Goovaerts, P., AvRuskin, G., Meliker, J., Slotnick, M., Jacquez, G.M., and J. Nriagu. 2005. Geostatistical modeling of the spatial variability of arsenic in groundwater of Southeast Michigan. Water Resources Research, 41(7), W07013 10.1029.

Gottschalk, L., 1993a. Correlation and covariance of runoff. Stochastic Hydrology and Hydraulics 7, 85-101.

Gottschalk, L., 1993b. Interpolation of runoff applying objective methods. Stochastic Hydrology and Hydraulics 7, 269-281.

Gottschalk L., Krasovskaia, I., 1998. Development of Grid-related Estimates of Hydrological Variables. Report of the WCP-Water Project B.3, Geneva, WCP/WCA, February 1998.

Gustard, A, Roald, L.A., Demuth, S., Lumadjeng, H.S., Gross, R., 1989. Flow Regimes from experimental and Network Data (FREND), Vol. 1, UNESCO, Paris.

Hawley, E.M., Mac Cuen, R.H., 1982. Water yield estimation in western United States. Journal of Irrigation and Drainage Division 108, 25-34.

Herschy, R.W., Fairbridge, R.W., 1998. Encyclopaedia of Hydrology and water resources, Kluwer Academic Publishers, Cambridge.

Huang, W.C., Yang, F.T., 1998. Streamflow estimation using Kriging. Water Resources Research 34, 1599-1608.

Journel, A.G., Huijbregts, C.J., 1978. Mining statistics, Academic Press, New York.

Jutman, T., 1995. Runoff. In Climate, lakes and rivers: National Atlas of Sweden, SNA Publishing, Stockholm, 106-111.

Krug, W.R., Gebert, W.A., Graczyk, D.J., Stevens, D.L., Rochelle, B.P., Church, M.R., 1990. Map of mean annual runoff for the northeastern, southeastern, and Mid-Atlantic United States, water years 1951–1980. U.S. Geol. Surv. Water Resour. Invest. Rep. 88-4094, Madison, WI.

Leblois, E., Sauquet, E., 2002. Grid elevation models in hydrology – Part 1: Principles and literature review; Part 2: HydroDEM, User's manual. Cemagref, Technical notes, Lyon.

Liebscher, H., 1972. A method for runoff-mapping from precipitation and air temperature data. Proceedings of the Symposium on world water balance (Gent Brugge, Belgium, 15-23 July 1970), AISH Publication n°92, vol. 1, 115-121.

Matérn, B., 1960. Spatial Variation. *Meddelanden från Statens Skogsforskiningsinstitut* 49(5).

Matheron, G., 1965. Les variables régionalisées et leur estimation. Une application de la théorie des fonctions aléatoires aux sciences de la nature. Ed. Masson, Paris (in French).

Merz, R., Blöschl, G., 2005. Flood frequency regionalisation – spatial proximity vs. catchment attributes. Journal of Hydrology 302, 283–306.

Pardé, M., 1955. Fleuves et rivières. Collection Armand Colin, Paris (in French).

Sauquet, E., Gottschalk, L., Leblois, E., 2000a. Mapping average annual runoff: A hierarchical approach applying a stochastic interpolation scheme. Hydrological Sciences Journal 45, 799-816.

Sauquet, E., Krasovskaïa, I., Leblois, E., 2000b. Mapping mean monthly runoff pattern using EOF analysis. Hydrology and Earth System Sciences 4, 79-93.

Shu, C., Burn, D., 2004. Artificial neural network ensembles and their application in pooled flood frequency analysis. Water Resources Research 40, doi: 10.1029/2003WR002816.

Solomon, S.I., Denouvilliez, J.P., Chart, E. J., Woolley, J. A., Cadou C., 1968. The use of a square grid system for computer estimation of precipitation, temperature, and runoff. Water Resources Research 4, 919-929.

Villeneuve, J.P., Morin, G., Bobee, B., Leblanc, D., Delhomme, J.P., 1979. Kriging in the Design of Streamflow Sampling Networks. Water Resources Research 15, 1833-1840.

Vogel, R.M., Wilson, I., Daly, C., 1999. Regional regression models of annual streamflow for the United States. Journal of Irrigation and Drainage Engineering 125, 148-157.

Wackerganel, H., 1995. Multivariate geostatistics. Springer Ed.

Figure captions

Fig. 1 The Garonne River at LAMAGISTERE (attributes in black) and the Girou River at CEPET (attributes in grey): catchment delineation, gauging stations (square) and centre of gravity (triangle), observed mean monthly runoff evaluated over the 1981-2000 period

Fig. 2 Observed mean monthly flow for several river basins in France evaluated over the 1981-2000 period

Fig. 3 Absolute difference between estimated and actual basin area, the basin is well reproduced if it is located below the black straight line which define the maximal deviation authorised by the tolerance criterion

Fig. 4 Studied regions and locations of the discharge stations (grey symbol denotes station with major karstic influences)

Fig. 5 Distribution of mean annual runoff generated by the sub-basins defined by the 898 gauging stations without or with not-pronounced karstic influence

Fig. 6 Variability of average annual runoff with mean elevation for Region 1, 4, 6 and 10

Fig. 7 Hypsometric curves of the ten studied regions

Fig. 8 Theoretical models and experimental semi-variogram of mean annual runoff $q\tilde{a}$ for Region 4 (c) and of residual ε_q to empirical formula including elevation for Regions 1, 6 and 10 (a, b and d)

Fig. 9 Map of mean annual runoff evaluated over the 1981-2000 period applying the hydro-stochastic approach

Fig. 10 Map of mean annual runoff for the French part of the Meuse basin over the 1981-2000 period

Fig. 11 Correction to the map of mean annual runoff nearby the Aroffe River to account for karst influence in discharge estimation: (a) details of the river network (black line) and the gauging stations (white square denotes the gauging station controlled by karst aquifer), (b) the derived discharge estimates, (c) correction by local ouflow and (d) the final map of mean annual river flow

Fig. 12 Map of mean annual flow along the river network over the 1981-2000 period

Fig. 13 Performance of the three geostatistical methods for regions 1, 4, 6 and 10 (full circle: hydro-stochastic approach, open triangle: residual kriging, cross: ordinary kriging using distance between centres of gravity)

Fig. 14 Performance of the three geostatistical methods considering all the stations: (a) scatter of predicted value versus observed ones and (b) distribution of the absolute error (full circle: hydro-stochastic approach, open triangle: residual kriging, cross: ordinary kriging using distance between centres of gravity, the black straight line indicate the one-to-one line)

Fig. 15 Box plots of absolute error for various classes of basin area (a: hydro-stochastic approach, b: residual kriging, c: ordinary kriging)

Tables

Table 1 Mean annual runoff $q\tilde{a}^*$ –elevation regressions. The number of gauged basins or sub-basins of adjacent regions included in the interpolation scheme is mentioned in brackets.

Region	*Number of stations*	*Intercept*	*Slope*	*Determination coefficient (%)*
1	110 (17)	1.29	23.8	63
2	46 (7)	0.93	207.2	18
3	132 (48)	0.93	82.2	48
4	154 (19)	0.73	252.6	5
5	218 (52)	0.36	209.2	35
6	209 (55)	0.42	260.7	40
7	35 (8)	0.58	350.3	50
8	89 (47)	1.01	58.1	58
9	64 (14)	0.36	492.1	38
10	149 (38)	0.35	196.8	47

Table 2 Variable to be mapped and parameters of the fitted exponential model for the semi-variogram

Region	*Variable under study*	*a (km)*	C_0 *(mm²)*
1	residual ε_q	20	29000
2	mean annual runoff $q\tilde{a}$	30	14000
3	residual ε_q	60	10000
4	mean annual runoff $q\tilde{a}$	70	27000
5	residual ε_q	30	35000
6	residual ε_q	25	55000
7	residual ε_q	70	160000
8	residual ε_q	50	55000
9	residual ε_q	40	130000
10	residual ε_q	60	60000

1 **Table 3** Summary statistics derived from the analysis of performance – for each statistic,

2 bold characters indicate the most efficient approach

		Hydro-stochastic approach					*Residual kriging*					*Ordinary Kriging*				
Region	*n*	*RMSE (mm)*	*MARE (%)*	*Slope*	*Int. (mm)*	*R² (%)*	*RMSE (mm)*	*MARE (%)*	*Slope*	*Int. (mm)*	*R² (%)*	*RMSE (mm)*	*MARE (%)*	*Slope*	*Int. (mm)*	*R² (%)*
1	87	**70**	**12**	**0.93**	**31**	**93**	81	14	0.91	51	91	101	18	0.84	89	85
2	14	51	14	0.90	25	60	**38**	**9**	0.85	39	**73**	44	10	**1.02**	**-11**	72
3	62	**35**	**12**	**0.88**	**27**	**94**	37	**12**	0.87	30	93	51	14	0.82	43	87
4	97	50	11	0.89	**27**	92	**42**	**10**	**0.92**	28	**94**	48	13	0.91	35	92
5	120	**65**	**10**	**0.86**	**47**	**88**	73	12	0.83	73	85	82	15	0.78	97	81
6	135	124	**16**	**0.80**	**88**	83	**121**	17	0.77	124	**84**	142	22	0.71	163	78
7	26	**88**	**8**	**0.96**	**4**	**97**	124	13	0.93	48	93	114	11	0.90	76	94
8	24	63	**8**	0.86	44	86	**60**	**8**	**0.88**	**40**	**87**	61	9	0.85	64	85
9	32	**128**	**10**	**0.77**	**216**	**89**	166	14	0.67	346	80	178	16	0.64	382	76
10	71	**96**	**17**	**0.92**	**19**	**85**	121	25	0.85	84	75	109	21	0.92	71	82
	668	**85**	**12**	**0.90**	**34**	**92**	94	14	0.88	57	90	103	17	0.86	73	88

3

Figures

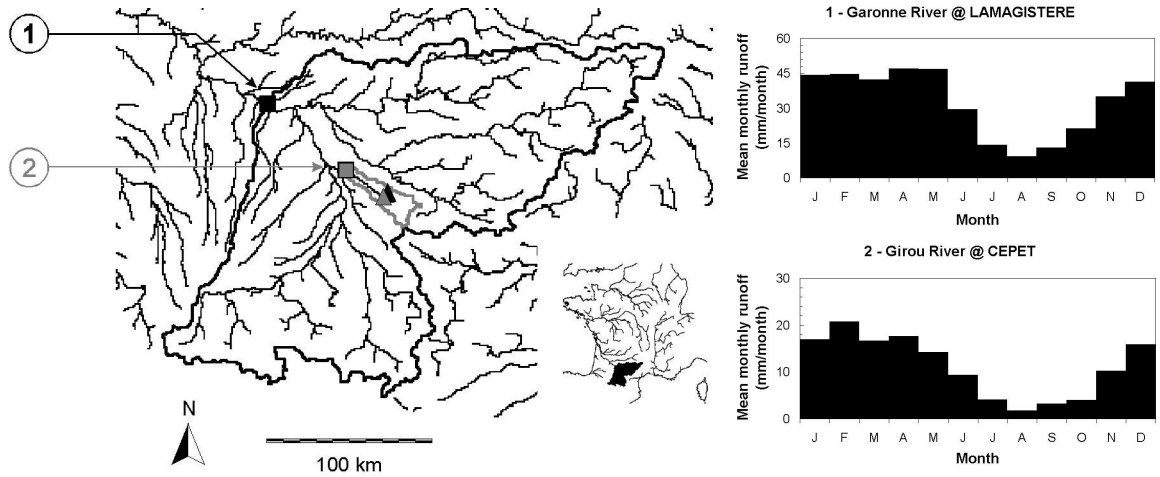

Figure 1

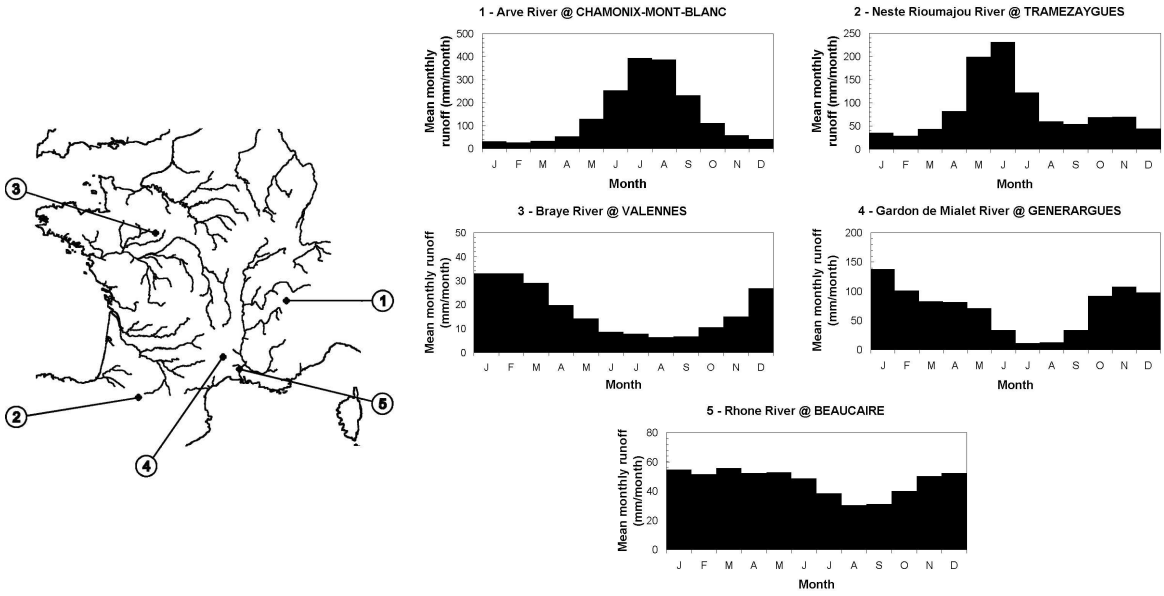

Figure 2

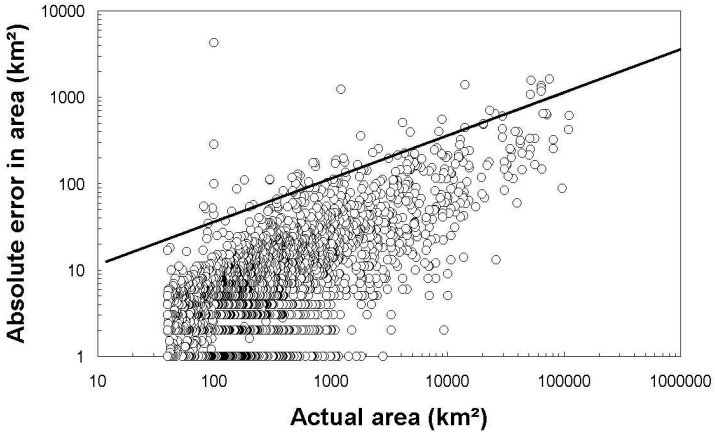

Figure 3

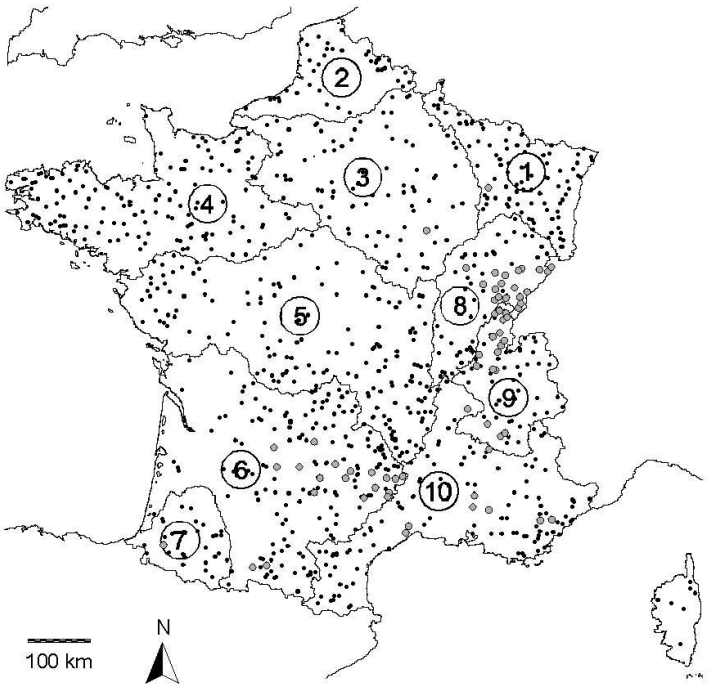

Figure 4

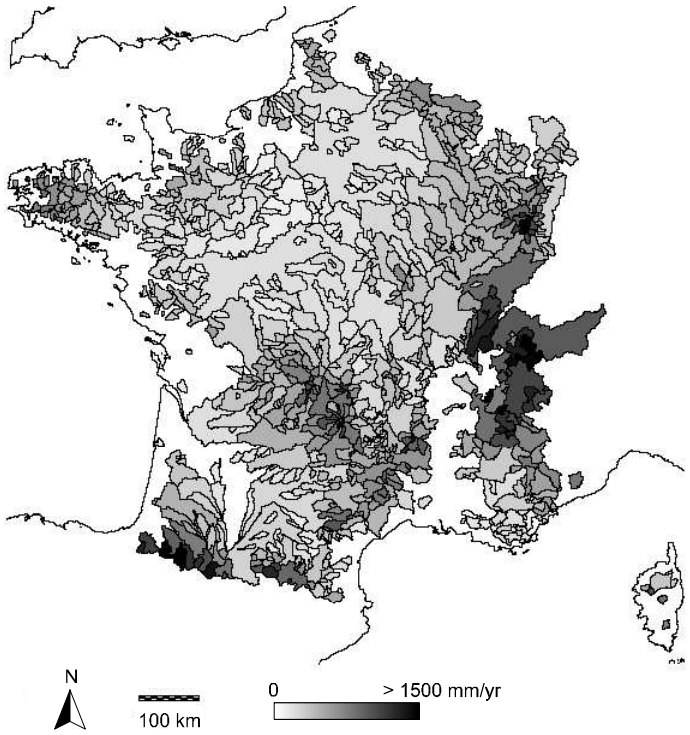

1

2 *Figure 5*

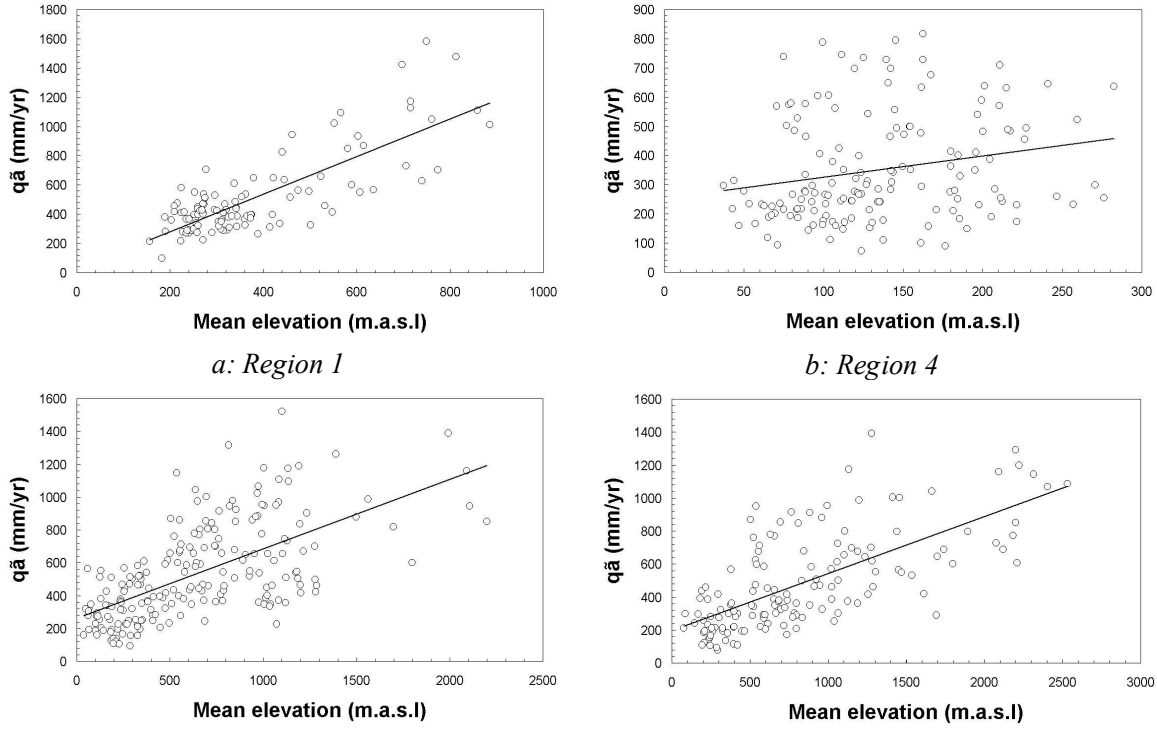

a: Region 1

b: Region 4

c: Region 6

d: Region 10

3 *Figure 6*

1

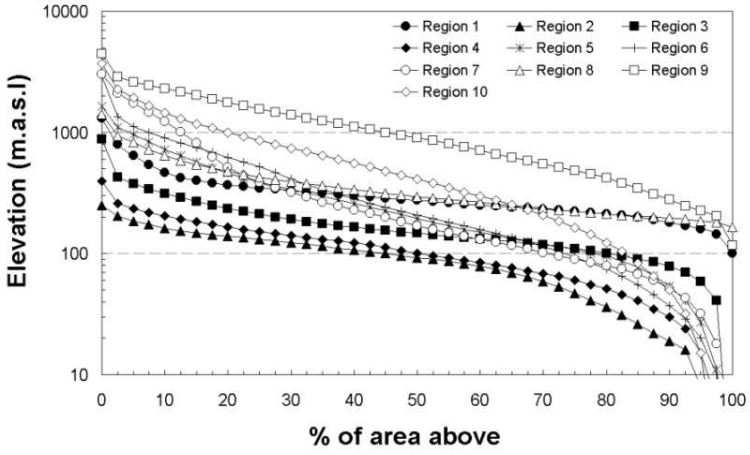

2

3 *Figure 7*

4

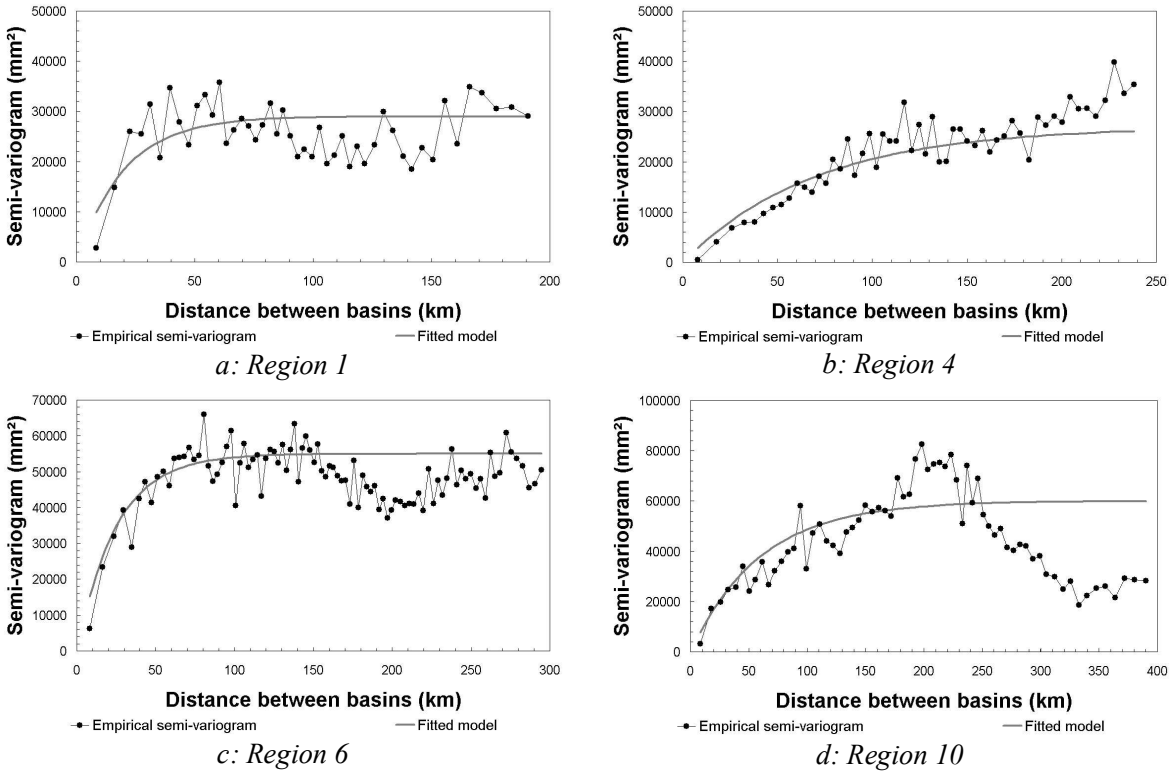

a: Region 1

b: Region 4

c: Region 6

d: Region 10

5 *Figure 8*

6

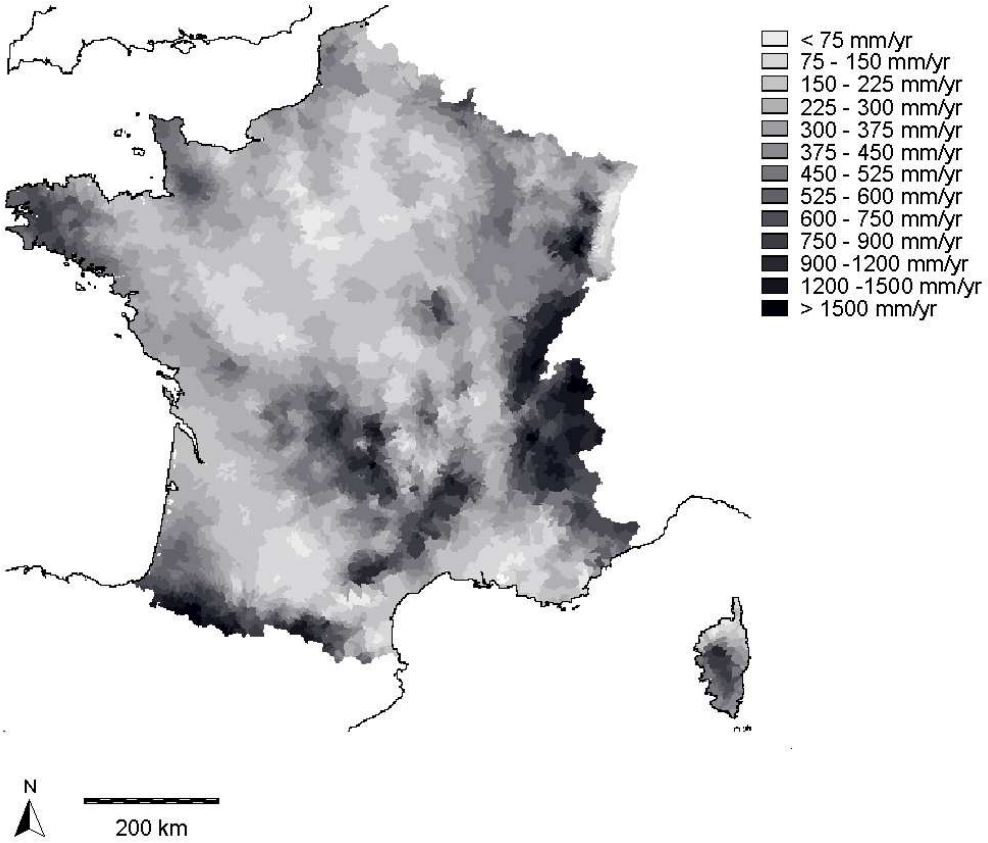

Figure 9

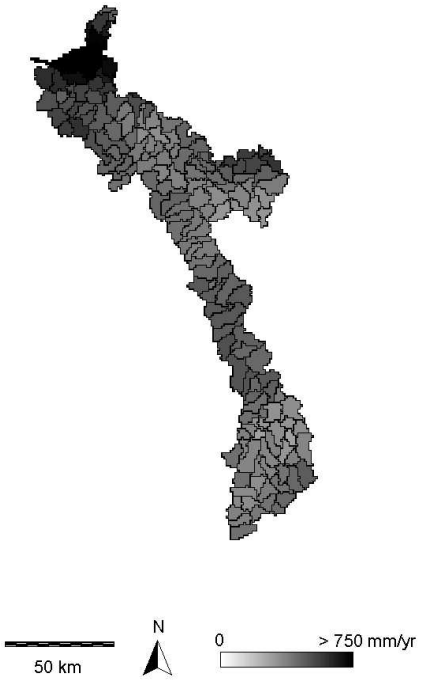

Figure 10

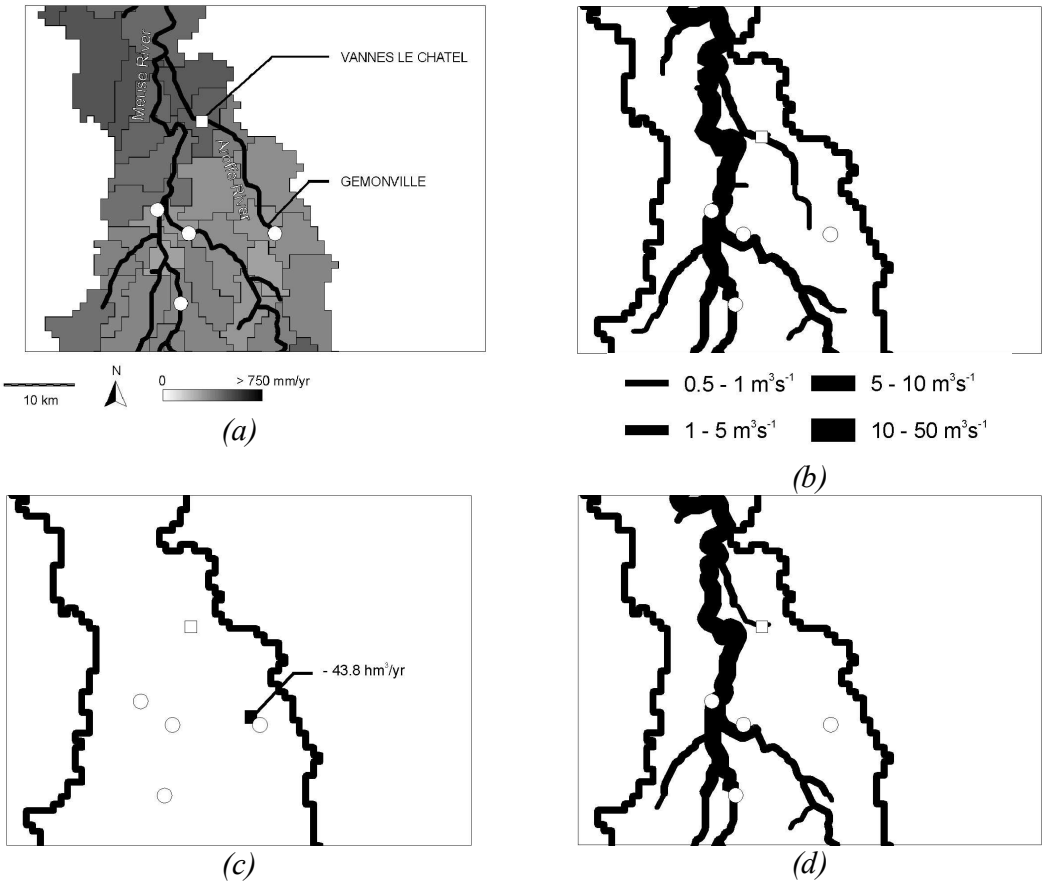

Figure 11

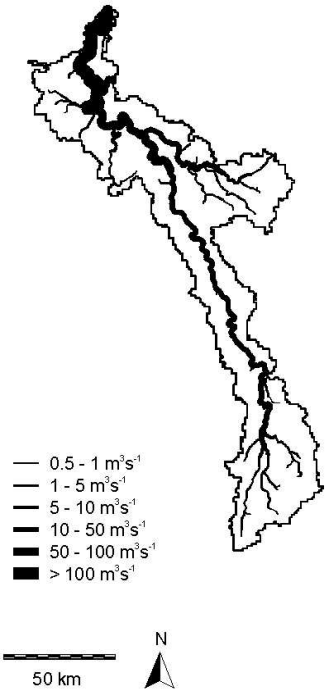

Figure 12

1

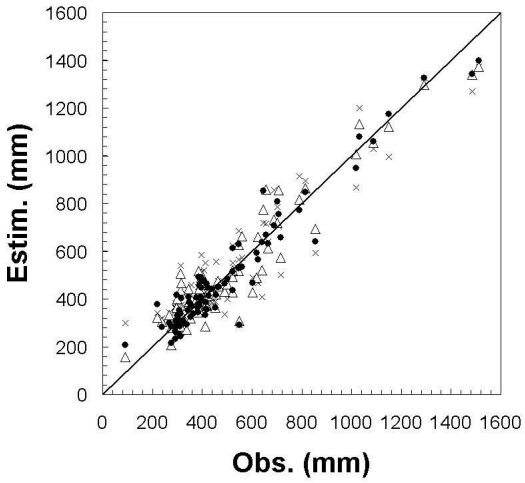

a : Region 1

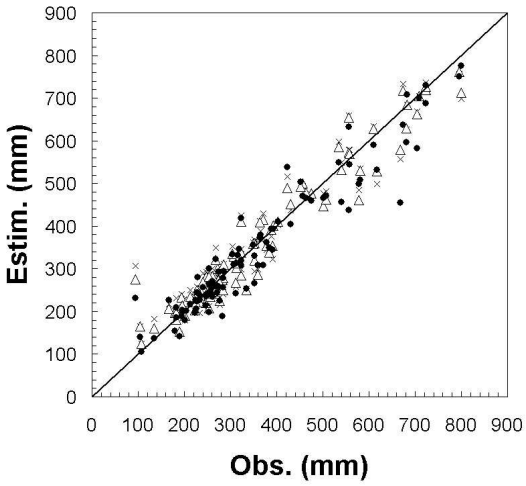

b: Region 4

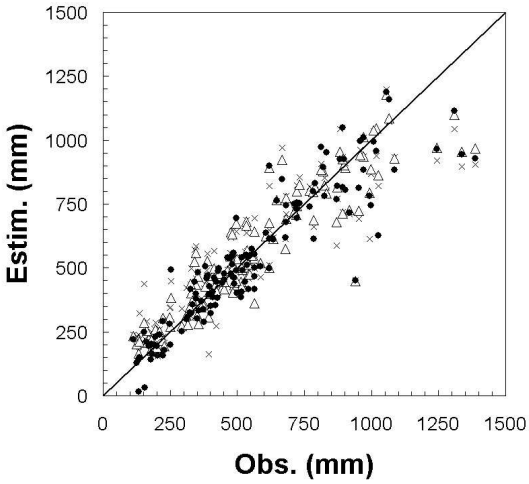

c: Region 6

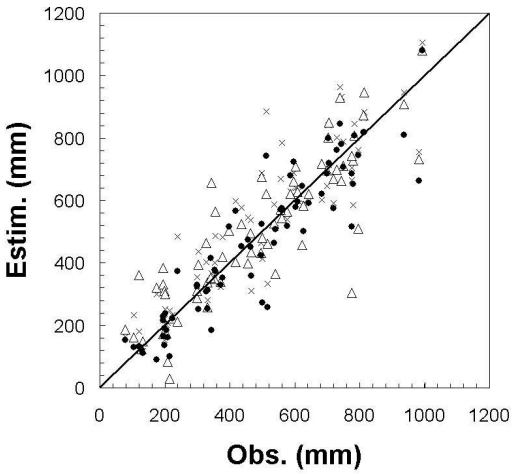

d: Region 10

2 *Figure 13*

3

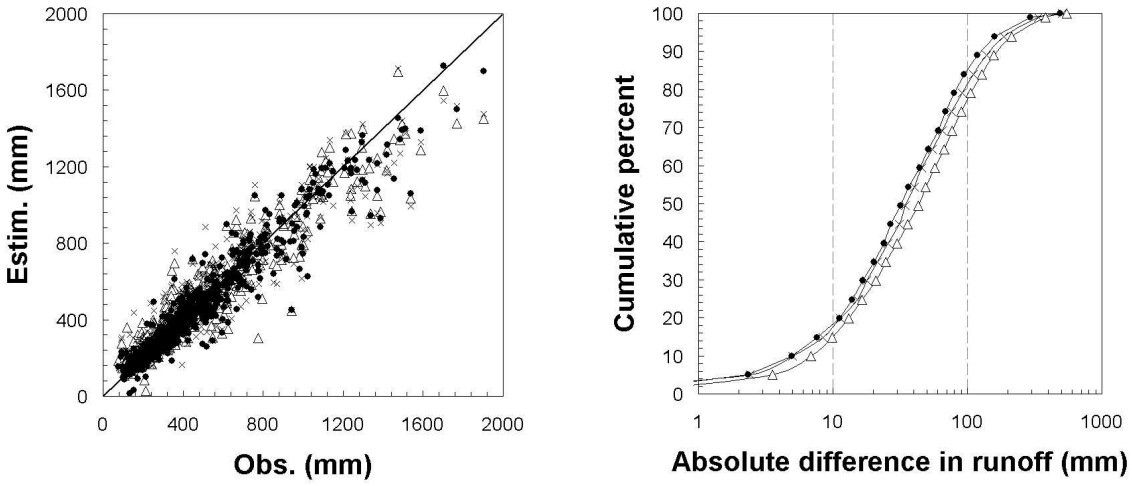

a *b*

Figure 14

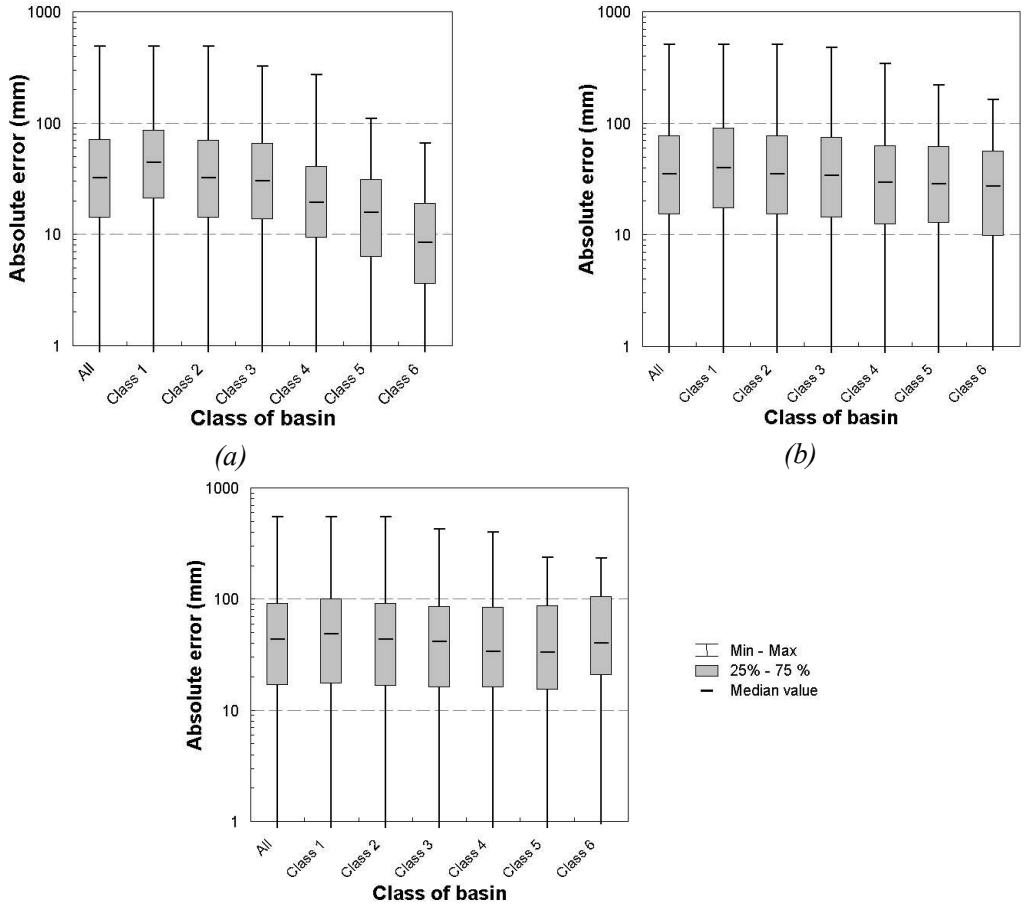

(a) *(b)*

(c)

Figure 15